



OPEN

Unusual derivatives from *Hypericum scabrum*

Sara Soroury^{1,2}, Mostafa Alilou³, Thomas Gelbrich⁴, Marzieh Tabefam², Ombeline Danton⁵, Samad N. Ebrahimi², Marcel Kaiser⁶, Matthias Hamburger⁵, Hermann Stuppner³ & Mahdi Moridi Farimani²✉

Three new compounds (1–3) with unusual skeletons were isolated from the *n*-hexane extract of the air-dried aerial parts of *Hypericum scabrum*. Compound 1 represents the first example of an esterified polycyclic polyprenylated acylphloroglucinol that features a unique tricyclo-[4.3.1.1⁴]-undecane skeleton. Compound 2 is a fairly simple MPAP, but with an unexpected cycloheptane ring decorated with prenyl substituents, and compound 3 has an unusual 5,5-spiroketal lactone core. Their structures were determined by extensive spectroscopic and spectrometric techniques (1D and 2D NMR, HRESI-TOFMS). Absolute configurations were established by ECD calculations, and the absolute structure of 2 was confirmed by a single crystal determination. Plausible biogenetic pathways of compounds 1–3 were also proposed. The *in vitro* antiprotozoal activity of the compounds against *Trypanosoma brucei rhodesiense* and *Plasmodium falciparum* and cytotoxicity against rat myoblast (L6) cells were determined. Compound 1 showed a moderate activity against *T. brucei* and *P. falciparum*, with IC₅₀ values of 3.07 and 2.25 μM, respectively.

Hypericum perforatum has gained great attention in the scientific community due to its high economic value, and prompted detailed phytochemical investigation into other *Hypericum* species^{1,2}. The *Hypericum* genus belonging to the Hypericaceae family with a wide distribution in temperate regions has been utilized in folk medicine of different parts of the globe^{1,3,4}. These plants are known to include several types of compounds such as prenylated acylphloroglucinols, terpenoids, flavonoids, xanthenes, naphthodianthrones^{5,6}, and some spiro compounds including spiroterpenoids⁷, spirolactones⁸, polyprenylated spirocyclic acylphloroglucinols⁹, and spiroketals¹⁰. These metabolites are also reported to display a wide range of pharmacological properties including antimicrobial, antitumor, antioxidant, anti-HIV, and antidepressant activities^{11–13}.

Hypericum scabrum has been used in Iranian folk medicine as an antiseptic, analgesic, sedative, and for treating headaches¹⁴. Prior phytochemical and pharmacological investigations into this species have demonstrated that the plant is rich in secondary metabolites, especially polycyclic polyprenylated acylphloroglucinols (PPAPs)^{15–18}. PPAPs are a class of synthetically challenging and structurally attractive natural compounds having an acylphloroglucinol-derived core modified with prenyl substituents, which display diverse pharmacological activities¹⁹. In course of a systematic exploration for new bioactive secondary metabolites with novel structure^{20–22}, three unprecedented structures (1–3, Fig. 1) were isolated from the aerial parts of *H. scabrum*. Although there are many examples of homo-adamantane PPAPs with a tricyclo[4.3.1.1^{5,7}]-undecane skeleton^{12,23,24}, compound 1 illustrates the first example of an esterified PPAP that features an unrivaled tricyclo-[4.3.1.1⁴]-undecane skeleton. Compound 2 is a reasonably simple monocyclic polyprenylated acylphloroglucinol (MPAP) with a unique cycloheptane ring decorated with prenyl substituents, and compound 3 has an unusual 5,5-spiroketal lactone core.

We here report on the structure elucidation of these compounds, including their absolute configuration, proposed biosynthetic pathways, and on the evaluation of their biological activity.

¹Department of Phytochemistry, Faculty of Science, Golestan University, 15759-49138 Gorgan, Iran. ²Department of Phytochemistry, Medicinal Plants and Drugs Research Institute, Shahid Beheshti University, Evin, Tehran, Iran. ³Institute of Pharmacy/Pharmacognosy, Center for Molecular Biosciences Innsbruck, University of Innsbruck, Innrain 80/82, 6020 Innsbruck, Austria. ⁴Institute of Pharmacy, Pharmaceutical Technology, University of Innsbruck, Innrain 52c, 6020 Innsbruck, Austria. ⁵Division of Pharmaceutical Biology, University of Basel, Klingelbergstrasse 50, 4056 Basel, Switzerland. ⁶Swiss Tropical and Public Health Institute, Socinstrasse 57, 4002 Basel, Switzerland. ✉email: m_moridi@sbu.ac.ir

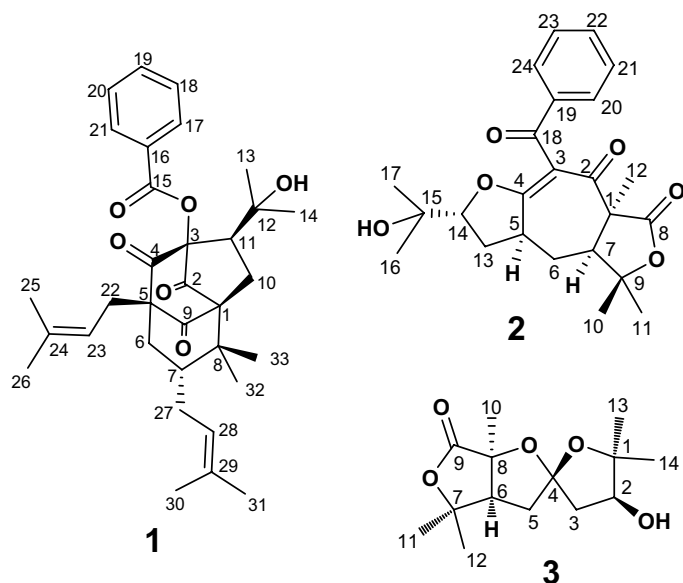


Figure 1. Structures of compounds 1–3.

Results and discussion

Compound **1** was obtained as yellow gum $\{[\alpha]_D^{25} + 17.2$ ($c = 1.0$, CH_3OH)}. Its molecular formula was deduced as $\text{C}_{33}\text{H}_{42}\text{O}_6$ by HR-ESIMS at m/z 535.3067 $[\text{M} + \text{H}]^+$ (calcd 535.3054), indicating 13 degrees of unsaturation. The ^1H NMR spectrum of **1** (Table 1) revealed signals of eight methyl singlets (δ_{H} 1.00, 1.05, 1.37, 1.46, 1.50, 1.54, 1.58, 1.65), two olefinic protons (δ_{H} 5.26, 1H, t, $J = 7.4$ Hz; 4.91, 1H, m), and a phenyl group (δ_{H} 7.87, 2H, dd, $J = 8.4, 1.2$ Hz; 7.51, 1H, t, $J = 7.5$ Hz; 7.36, 2H, t, $J = 7.8$ Hz). Analysis of the ^{13}C NMR (Table 1) and HSQC spectra of **1** exhibited 33 carbon signals comprising three carbonyl groups [δ_{C} 203.3, 201.4, 200.9], a benzoate group [δ_{C} 165.6, 134.0, 129.9 \times 2, 128.7 \times 2, 127.9], eight methylenes, four methines, and six quaternary carbons. The aforementioned data indicated some structural aspects of 7-*epi*-clusianone (**4**, Fig. 5), a BPAP with a normal bicyclo[3.3.1]-nonane core²⁵, that was also isolated in this study²⁶. The main spectral differences between **1** and **4** were due to the significant variations in the NMR data of the perenyl group at C-1, replacement of a benzylic ketone at δ_{C} 197.7 with a benzylic ester at δ_{C} 165.6, and replacement of an enolic carbon at δ_{C} 196.5 with a ketonic one at δ_{C} 200.9. Detailed analysis of the ^1H and ^{13}C NMR spectra indicated that a $[\text{CHC}(\text{CH}_3)_2\text{OH}]$ group in **1** replaced the isobutenyl moiety at C₁₀ in **4**. This deduction was corroborated by the key HMBC correlations from H₃-13 (δ_{H} 1.37) and H₃-14 (δ_{H} 1.46) to C-12 (δ_{C} 75.0) and C-11 (δ_{C} 45.4), coupled with the ^1H - ^1H COSY correlation between H-11 (δ_{H} 2.11) and H₂-10 (δ_{H} 1.92 and 1.98), as shown in Fig. 2. Additionally, HMBC correlations from H-11 to C-3 (δ_{C} 89.5), C-4 (δ_{C} 200.9), C-2 (δ_{C} 201.4), and from H₂-10 to C-3 and C-8 (δ_{C} 46.3), demonstrated the foundation of a five-membered ring by the connection of C-11 to C-3. In the HMBC spectrum, correlations from aromatic protons (δ_{H} 7.87) to the resonance of a carbonyl group at (δ_{C} 165.6), supported by the upfield shift of C-3 resonance (δ_{C} 89.5) compared to it at **4** (δ_{C} 115.9), suggested the displacement of a benzoate ester at C-3 instead of the phenyl ketone. Moreover, HMBC correlations from H₂-22 and H₂-6 to the carbonyl resonances at δ_{C} 200.9 and δ_{C} 203.3 confirmed the position of the two other ketone groups at C-4 and C-9. The remaining parts of the molecule were similar to those of **4**. Thus, the gross structure of **1** was established as depicted in Fig. 1.

The NOESY spectrum (Fig. 3) demonstrated correlations from H-7 to H-6 β and H₃-33, and from H₃-33 to H-10 β and certified their cofacial orientation. Also, diagnostic cross-peaks from H-27 α to H₃-32 and H-6 α , from H₃-32 to H-10 α , and from H-10 α to H-11, revealed their equal orientation. The absolute stereochemistry was specified by comparing the calculated ECD spectra with the experimental one. The experimental data showed two positive Cotton effects (CE) at 280 and 205 nm, along with negative CE at 220 nm (Fig. 4). The calculated ECD spectrum for 1*R*, 3*S*, 5*S*, 7*R*, 11*R* showed a good compatibility with the experimental data.

The hypothetical biogenetic pathway of **1** is proposed in Fig. 5. 7-*epi*-clusianone (**4**), an *endo*-bicyclic polyperenylated acylphloroglucinol (*endo*-BPAP) is assumed to be a precursor. The structural novelty of **1** involves ring closure of the enone moiety upon the epoxy function of the prenyl chain at C-1, to form a rigid caged tetracyclo-[4.3.1.1^{1,4}]-undecane skeleton. Furthermore, a Baeyer–Villiger oxidation is required to create **1** as the first esterified PPAP in nature.

Compound **2** was obtained as a white powder $\{[\alpha]_D^{25} + 30.5$ ($c = 1.0$, CHCl_3)}. Its molecular formula was distinguished as $\text{C}_{24}\text{H}_{28}\text{O}_6$ by HR-ESIMS at m/z 413.1941 $[\text{M} + \text{H}]^+$ (calcd 413.1959), proposing 11 degrees of unsaturation. The ^1H NMR spectrum of **2** (Table 1) displayed signals of a mono-substituted phenyl group (δ_{H} 7.77, 2H, dd, $J = 8.3, 1.2$ Hz; 7.46, 1H, t, $J = 7.4$ Hz; 7.35, 2H, t, $J = 7.7$ Hz), five methyl singlets (δ_{H} 1.05, 1.12, 1.20, 1.39, 1.77), two diastereotopic methylenes [$(\delta_{\text{H}}$ 1.83, 1H, m; 2.13, 1H, ddd, $J = 13.7, 6.9, 1.7$ Hz); and (δ_{H} 1.90, 1H, ddd, $J = 12.9, 11.0, 9.2$ Hz; 2.52, 1H, ddd, $J = 12.9, 9.0, 1.2$ Hz)], and three methines including one oxygenated

| No. | 1 | | No. | 2 | |
|-------------|------------|---------------------|-------------|------------|----------------------------|
| | δ_C | δ_H , mult | | δ_C | δ_H , mult |
| 1 | 72.6 | | 1 | 62.4 | |
| 2 | 201.4 | | 2 | 193.7 | |
| 3 | 89.5 | | 3 | 113.5 | |
| 4 | 200.9 | | 4 | 179.0 | |
| 5 | 64.9 | | 5 | 40.8 | 3.61 m |
| 6 α | 36.1 | 1.85 d (14.6) | 6 α | 31.6 | 2.13 ddd (13.7, 6.9, 1.7) |
| 6 β | | 2.45 dd (14.6, 6.5) | 6 β | | 1.83 m |
| 7 | 41.8 | 2.05 t (7.4) | 7 | 55.0 | 2.43 dd (12.1, 6.9) |
| 8 | 46.3 | | 8 | 174.1 | |
| 9 | 203.3 | | 9 | 83.6 | |
| 10 α | 26.9 | 1.98 ^a | 10 | 23.6 | 1.20 s |
| 10 β | | 1.92 ^a | | | |
| 11 | 45.4 | 2.11 dd (10.7, 8.5) | 11 | 28.5 | 1.39 s |
| 12 | 75.0 | | 12 | 26.1 | 1.77 s |
| 13 | 27.7 | 1.37 s | 13 α | 32.1 | 2.52 ddd (12.9, 9.0, 1.2) |
| | | | 13 β | | 1.90 ddd (12.9, 11.0, 9.2) |
| 14 | 31.2 | 1.46 s | 14 | 90.1 | 4.25 dd (9.2, 1.2) |
| 15 | 165.6 | | 15 | 72.6 | |
| 16 | 127.9 | | 16 | 26.3 | 1.12 s |
| 17,21 | 129.9 | 7.87 dd (8.4, 1.2) | 17 | 26.4 | 1.05 s |
| 18,20 | 128.7 | 7.36 t (7.8) | 18 | 193.5 | |
| 19 | 134.0 | 7.51 t (7.5) | 19 | 137.3 | |
| 22 | 28.7 | 2.53 ^c | 20,24 | 128.9 | 7.77 dd (8.3, 1.2) |
| 23 | 119.3 | 5.26 t (7.4) | 21,23 | 128.5 | 7.35 t (7.7) |
| 24 | 134.8 | | 22 | 133.2 | 7.46 t (7.4) |
| 25 | 26.0 | 1.65 s | | | |
| 26 | 18.0 | 1.58 s | | | |
| 27a | 25.5 | 2.42 dd (12.9, 5.2) | | | |
| 27b | | 2.53 ^a | | | |
| 28 | 120.0 | 4.91 tq (5.7, 1.2) | | | |
| 29 | 131.9 | | | | |
| 30 | 25.9 | 1.50 s | | | |
| 31 | 17.8 | 1.54 s | | | |
| 32 | 25.3 | 1.00 s | | | |
| 33 | 23.4 | 1.05 s | | | |

Table 1. ¹H and ¹³C NMR data (CDCl₃) of **1** (¹H (500 MHz) and ¹³C (125 MHz)) and **2** (¹H (600 MHz) and ¹³C (150 MHz).) (δ in ppm, J in Hz). ^aOverlapping signals.

(δ_H 2.43, 1H, dd, J = 12.1, 6.9 Hz; 3.61, 1H, m; 4.25, 1H, dd, J = 9.2, 1.2 Hz). The ¹³C spectrum of **2** (Table 1) showed 24 carbon signals including five methyls, two methylenes, eight methines (five aromatics) and nine quaternary carbons (one aromatic). Accordingly, 27 protons could be numerated, while the unaccounted one could be due to the presence of an OH substituent in the structure. Deshielded ¹³C NMR resonances at δ_C 193.7 (C-2), 113.5 (C-3), and 179.0 (C-4) proposed the attendance of an α,β -unsaturated ketone moiety comprising a tetrasubstituted olefinic group and an oxygen substituent at the β -position. The resonances at δ_C 174.1 (C-8) and 193.5 (C-18) were indicative of two other carbonyl groups. Three carbon signals at δ_C 72.6 (C-15), 83.6 (C-9), and 90.1 (C-14) indicated the entity of oxygenbearing sp^3 carbons. Considering the number of sp^2 or sp carbon resonances and 11 degrees of hydrogen deficiency, a tricyclic core structure for compound **2** was clearly deduced that possesses a seven-membered carbocyclic ring, a cyclic ether and a lactone moiety. By interpreting COSY correlations (Fig. 2), it was thinkable to create a long proton connection from H-7 to H-14 through H₂-6, H-5, and H₂-13. The HMBC spectrum showed correlations from H-5 to C-3, C-4, C-6, and C-7, and from H-7 to C-1 and C-2, proving the seven-member carbocyclic ring as the core of the structure. HMBC correlations from H-14 to C-4, C-15, C-16, and C-17 resulted in the construction of the ether ring with a substituted 2-propanol moiety. HMBC cross-peaks from H₃-10 and H₃-11 to C-9 and C-7, and from H-7 to C-9, corroborated the nature of the lactone moiety. The fifth methyl group was placed at C-1 pursuant to the HMBC cross-peaks of H₃-12 with C-1, C-2, C-7, and C-8. In the HMBC spectrum, correlations from aromatic protons (δ_H 7.77) to the resonance of a carbonyl group at (δ_C 193.5) supported the presence of the benzoyl moiety at C-3. However, no direct HMBC correlations to C-3 were observed.

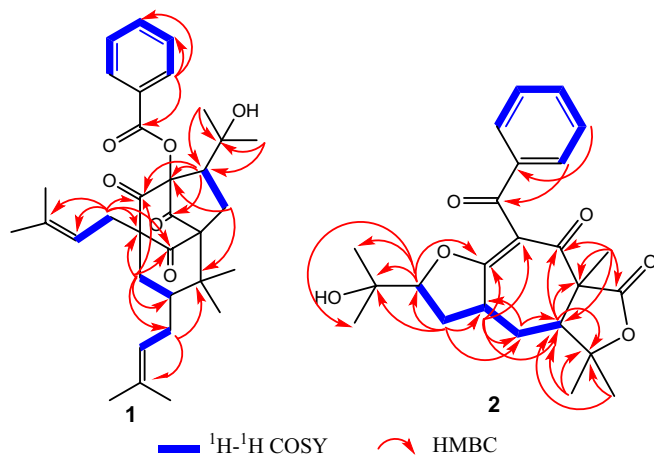


Figure 2. ^1H - ^1H COSY and key HMBC correlations of **1** and **2**.

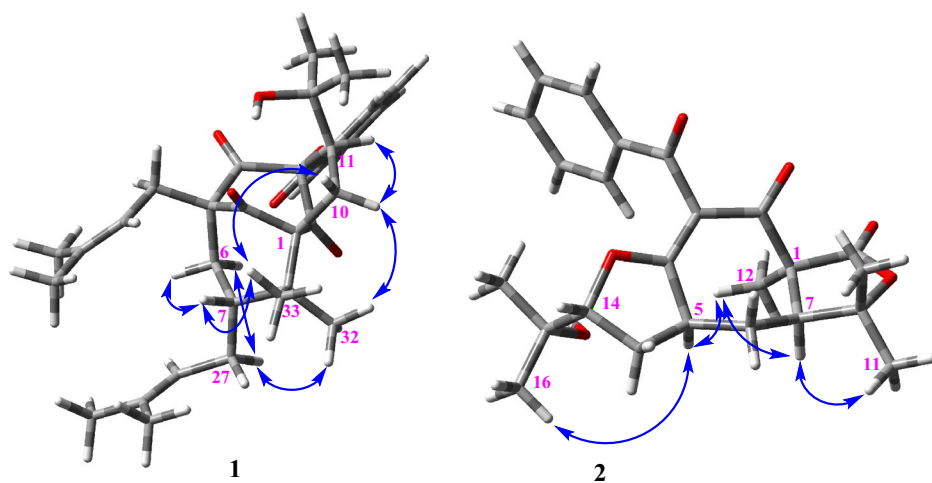


Figure 3. NOESY correlations of **1** and **2**.

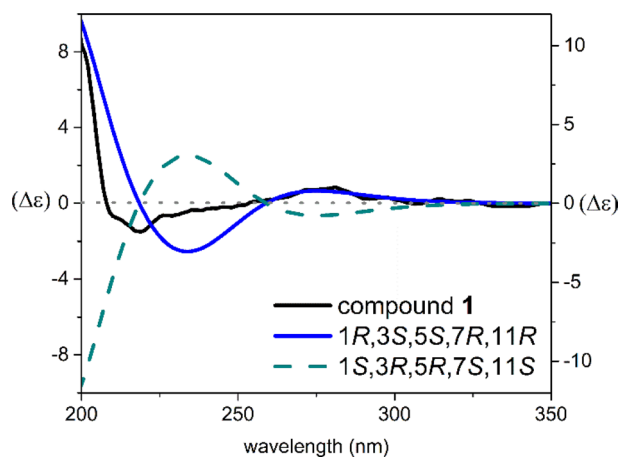


Figure 4. Comparison of experimental and TDDFT calculated ECD spectra of **1**.

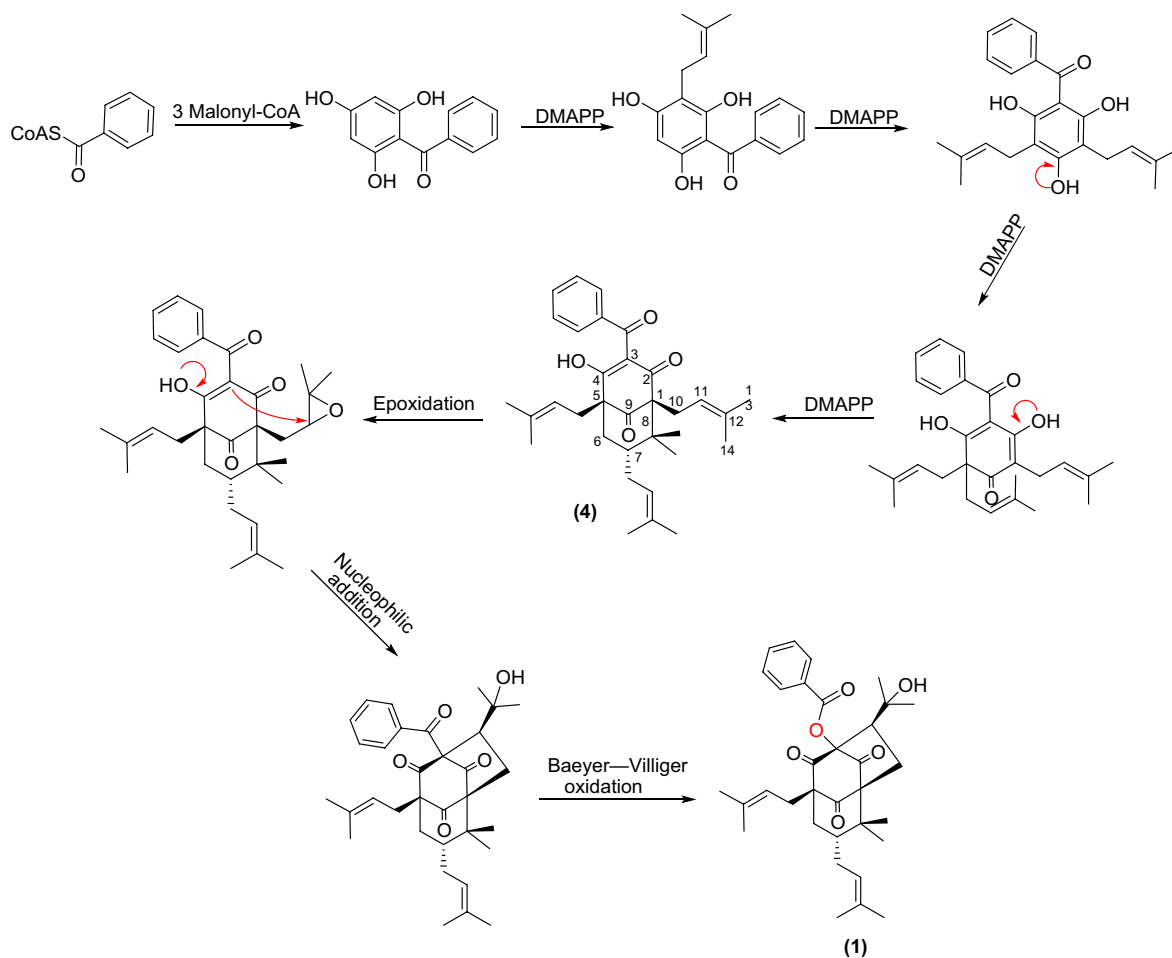


Figure 5. Putative biosynthetic pathway to **1**.

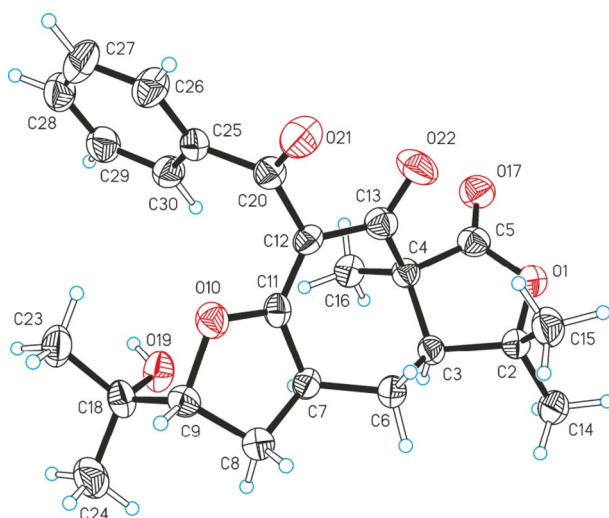


Figure 6. Molecular structure of **2** (non-H atoms are represented as thermal ellipsoids drawn at the 50% level).

The relative stereochemistry of **2** was resolved by inspecting the NOESY spectrum (Fig. 3). In the NOESY spectrum, H₃-12 showed NOE correlations with H-7 and H-5, indicating their α -orientations. The fact that no NOE correlation peaks were found between H-5 and H-14, and instead, a cross-peak was detected between H-5 and H₃-16, indicated the β orientation of H-14. Conclusive evidence for the postulated structure of **2** was

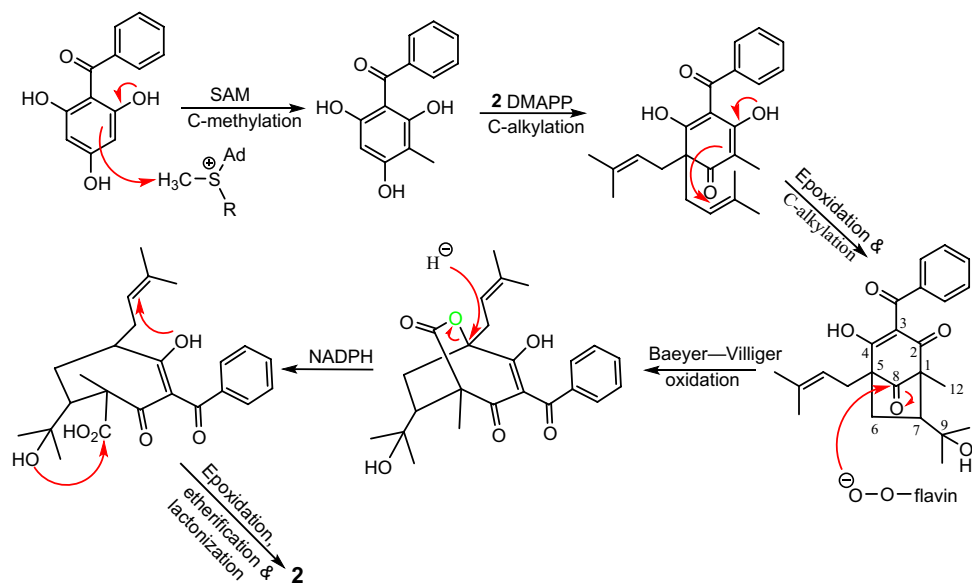


Figure 7. Putative biosynthetic pathway to **2**.

| No | C_5D_5N | | $CDCl_3$ | |
|------------|------------|---------------------|------------|---------------------|
| | δ_c | $\delta_{H, mult}$ | δ_c | $\delta_{H, mult}$ |
| 1 | 85.8 | | 85.5 | |
| 2 | 76.5 | 4.37 dd (5.7, 3.9) | 77.3 | 4.01 dd (5.8, 3.2) |
| 3 α | 43.7 | 2.54 dd (14.2, 5.8) | 43.0 | 2.25 dd (14.5, 5.9) |
| 3 β | | 2.48 dd (14.2, 3.9) | | 2.02 ^a |
| 4 | 110.6 | | 110.0 | |
| 5 α | 32.4 | 2.30 m | 32.2 | 2.01 ^a |
| 5 β | | 2.38 dd (9.5, 2.1) | | 2.01 ^a |
| 6 | 47.0 | 2.32 m | 47.3 | 2.03 ^a |
| 7 | 83.6 | | 83.4 | |
| 8 | 84.7 | | 84.5 | |
| 9 | 172.7 | | 171.9 | |
| 10 | 22.7 | 1.83 s | 22.9 | 1.65 s |
| 11 | 23.8 | 1.35 s | 24.3 | 1.41 s |
| 12 | 29.5 | 1.22 s | 30.0 | 1.34 s |
| 13 | 27.5 | 1.40 s | 27.0 | 1.21 s |
| 14 | 23.0 | 1.55 s | 22.3 | 1.21 s |

Table 2. 1H (500 MHz) and ^{13}C (125 MHz) NMR data (C_5D_5N and $CDCl_3$) of **3** (δ in ppm, J in Hz).
^aOverlapping signals.

obtained from a single-crystal X-ray structure analysis, which precisely confirmed the absolute configuration as (1*S*, 5*S*, 7*S*, 14*R*) (Fig. 6).

Many bi- and tricyclic PPAPs have been reported to occur in nature, however compound **2** is the first monocyclic polyprenylated acylphloroglucinol (MPAP) with a cycloheptane ring decorated with prenyl substituents.

Biosynthetically, compound **2** is presumably derived from a common phloroglucinol core (Fig. 7) via methylation at C-1 and diprenylation at C-5, followed by the C-alkylation of the epoxide intermediate to form the C₁–C₇ bond. This intermediate contains a bicyclo[3.2.1]octane-2,4,8-trione core that was found in a smaller group of PPAPs²⁷. A Baeyer–Villiger oxidation, followed by a ring opening through the nucleophilic attachment of NADPH, would then form the cycloheptane key ring. Finally, successive formation of the hydrofuran and lactone rings via etherification and lactonization of the side chains would lead to compound **2**.

Compound **3**, colorless oil $\{[\alpha]_D^{25} + 9.1$ ($c = 1.0$, CH_3OH) $\}$, showed an accurate HR-ESIMS ion at m/z 293.1366 $[M + Na]^+$ (calcd 293.1365), revealing the molecular formula as $C_{14}H_{22}O_5$ and four indices of hydrogen deficiency. 14 carbon resonances can be observed from the ^{13}C NMR spectrum of **3** (Table 2), corresponding to five methyls, two methylenes, two methines and five quaternary carbons. Accordingly, twenty-one of the hydrogens were

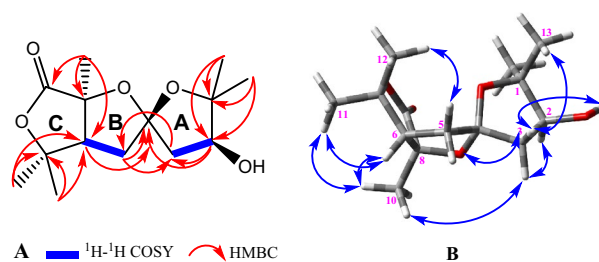


Figure 8. (A) ^1H - ^1H COSY and key HMBC and (B) NOESY correlations of **3**.

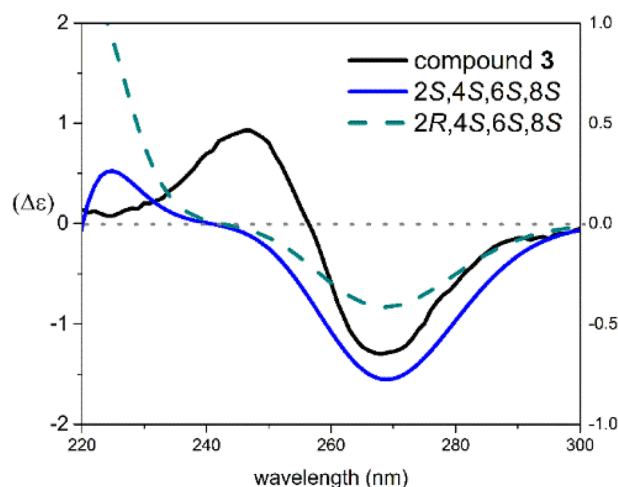


Figure 9. The experimental and TDDFT calculated ECD spectra of **3**.

carbon-bonded, so the remaining one could belong to a hydroxyl group. The ^{13}C NMR spectrum displayed signals suggestive of a carbonyl carbon (δ_{C} 172.7) and four oxygenbearing carbons [δ_{C} 76.5 (CH), 83.6 (C), 84.7 (C) and 85.8 (C)]. The lack of any other olefinic carbon signals indicated that **3** contains three heterocycle rings, to fulfill its degrees of unsaturation. The ^1H NMR (Table 2) spectrum of **3** recorded in $\text{C}_5\text{D}_5\text{N}$ revealed the distinguished resonances of five methyl singlets (δ_{H} 1.22, 1.35, 1.40, 1.55, 1.83), two diastereotopic methylenes [(δ_{H} 2.30, 1H, m; 2.38, 1H, dd, $J=9.5$, 2.1 Hz); and (δ_{H} 2.48, 1H, dd, $J=14.2$, 3.9 Hz; 2.54, 1H, dd, $J=14.2$, 5.8 Hz)], and two methines including one oxygenated (δ_{H} 4.37, dd, $J=5.7$, 3.9 Hz) and one nonoxygenated (δ_{H} 2.32, m). The partial structure of **3** was established from a combination of HSQC, ^1H - ^1H COSY, and HMBC experiments in $\text{C}_5\text{D}_5\text{N}$ and CDCl_3 . HMBC correlations from H_3 -11 and H_3 -12 to C-7 and C-6, and from H_3 -10 to C-6, C-8, and C-9, corroborated the constitution of the lactone ring. HMBC cross-peaks of H-6 and H_2 -5 with C-4 confirmed the attendance of a five-membered heterocyclic ring B. HMBC data (correlations from H_3 -13 and H_3 -14 to C-1 and C-2, and from H-2 to C-3 and C-4) revealed the connectivity between C_1 - C_2 - C_3 - C_4 as ring A (Fig. 8). Finally, correlations of H_2 -3 with C-5, and of H_2 -5 with C-3, implied that the C-4 tertiary carbon was a bridgehead between C-3 and C-5 as a spiroketal.

The NOESY spectrum (Fig. 8) represented correlations between H-6, H_3 -10 and H_3 -11, as well as between H_3 -12 and H-5 β , which emphasized the connection of rings B and C. Similarly, cross-peaks between H_3 -10 and H-3 α , between H-5 α and H-3 β , between H-3 α and H-2, as well as between H-3 β and H_3 -13, were noticed and confirmed the linkage of rings A and B. The ECD spectrum of compound **3** showed a negative Cotton effect (CE) at 275 nm and a positive CE at 250 nm. Comparing the experimental ECD curve of **3** with calculated one resulted in deciphering the absolute stereochemistry of **3** as 2S, 4S, 6S, 8S (Fig. 9).

Isolation of **3** with intriguing 5,5-spiroketal lactone structure represents the first discovery from nature. From a biogenetic viewpoint, acetate and mevalonate pathways might be involved in the biosynthesis of this new scaffold. Although two isoprene C_5 units appear to be involved in this process, it does not seem to fit the regular alkylation mechanism (Fig. 10).

Compounds **1**-**3** were examined for their in vitro antiprotozoal activity against the protozoan parasites *Trypanosoma brucei rhodesiense* and *Plasmodium falciparum*. Cytotoxicity was investigated in rat skeletal myoblast L6 cells and the selectivity indices (SI) for these compounds were calculated (Table 3).

Four known polycyclic polyprenylated acylphloroglucinols hyperibone A-C^{15a} and 7-*epi*-clusianone²⁵, and two aromadendrane sesquiterpenoids lochmolin F²⁸ and aromadendrane-4 β ,10 β -diol²⁹ were also isolated and identified in this study. Hyperibone A-C have been previously reported from the aerial parts of the plant, but the remainings were isolated for the first time from this species.

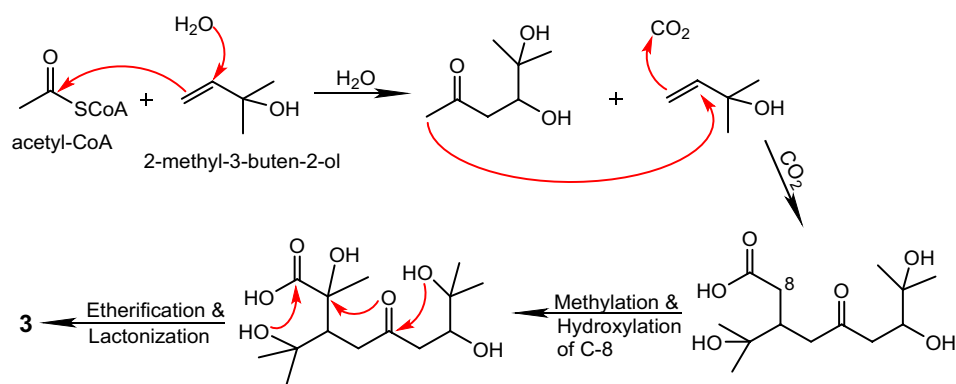


Figure 10. Putative biosynthetic pathway to **3**.

| Compound | IC ₅₀ (μM) ^a | | |
|-----------------|------------------------------------|----------------------------------|--------------|
| | <i>T. b. rhodesiense</i> | <i>P. falciparum</i> | L6 cells |
| 1 | 3.07 ± 0.77; 11.07 ^b | 2.25 ± 0.10; 15.10 ^b | 33.98 ± 2.16 |
| 2 | > 100.0 | > 100.0 | > 100.0 |
| 3 | > 100.0 | 21.14 ± 1.60; 17.50 ^b | > 100.0 |
| Melarsoprol | 0.04 | | |
| Chloroquine | | 0.01 | |
| Podophyllotoxin | | | 0.009 |

Table 3. In vitro activity of compounds 1–3 against *T. b. rhodesiense* (STIB900) and *P. falciparum* (NF54) and cytotoxicity in L6 Cells. ^aAverage of at least two independent assays. ^bSelectivity index (SI): IC₅₀ in L6 cells divided by IC₅₀ in the titled parasitic strain.

Methods

General experimental procedures. Optical rotation, UV and ECD spectra, and HR-ESIMS data were recorded as reported previously by us³⁰. NMR experiments were measured on Bruker Avance III 500 and Bruker Avance II 600 spectrometers, using standard Bruker pulse sequences. HPLC separations were performed on a Knauer HPLC system according to our previous report³⁰. Column chromatography (CC) was carried out on silica gel (70–230 mesh, Merck). TLC pre-coated silica gel F₂₅₄ plates (Merck) were used to detect and merge fractions; visualizing under UV light or by heating the plates after spraying with anisaldehyde-sulfuric acid reagent.

Plant material. The aerial parts of *H. Scabrum* were gathered in the north of Iran in Yush village from Baladeh District, in June 2015. A voucher specimen was authenticated by Dr. Ali Sonboli and was deposited in the Herbarium of the Medicinal Plants and Drugs Research Institute, Shahid Beheshti University (MPH-2510).

Extraction and isolation. After drying and powdering, the-aerial parts of *H. scabrum* (5.0 kg) were extracted (3 × 20 L, 24 h) with *n*-hexane, and the mixed extracts were condensed under vacuum to give a gummy residue (150 g). The dried extract was fractionated by open column chromatography on silica gel (1.0 kg, 5 × 100 cm, 70–230 mesh) eluted with a gradient of *n*-hexane–EtOAc (100:0 to 0:100), and then increasing amounts of MeOH (up to 50%). On the bases of TLC analysis, eight combined fractions (Fr.1–Fr.8) were obtained. From Fr.1 [eluted with *n*-hexane–EtOAc (95:5)] a yellow crude solid was obtained, which was triturated with MeOH to give 7-*epi*-clusianone (**4**) as white powder (100 mg). Fr.2 (1.0 g) was further purified on silica gel column chromatography (200 g, 2 × 60 cm) and eluted with *n*-hexane–CH₂Cl₂–(CH₃)₂CO (58:40:2) to get four subfractions (Fr.2.1–Fr.2.4). Fr.2.2 (70 mg) was subjected to silica gel column (70 g, 1 × 50 cm) eluted with *n*-hexane–(CH₃)₂CO (90:10) to afford compound **1** (7.0 mg). Fr.2.3 (150 mg) was submitted to a silica gel column (140 g, 1.5 × 70 cm), eluted with *n*-hexane–(CH₃)₂CO (80:20) to obtain two subfractions (Fr.2.3a–Fr.2.3b). Repeated purification of Fr.2.3a (80 mg) by silica gel CC [100 g, 1 × 70 cm, eluted with CH₂Cl₂–(CH₃)₂CO (97:3)], afforded hyperibone A (2.5 mg), hyperibone B (1.5 mg) and hyperibone C (14 mg). Fr.4 (1.9 g) was further separated via silica gel column chromatography (300 g, 4 × 60 cm) using CH₂Cl₂–(CH₃)₂CO (95:5) as eluent to produce five subfractions (Fr.4.1–Fr.4.5). Fr.4.1 (170 mg) was further chromatographed on silica gel (150 g, 1.5 × 80 cm) using CH₂Cl₂–1-propanol–MeOH (95:4:1) as mobile phase to yield lochmolin F (5.7 mg) and aromadendrane-4β,10β-diol (2 mg). Fr.4.3 (100 mg) was also separated on silica gel (120 g, 1.5 × 50 cm) and eluted with *n*-hexane–(CH₃)₂CO (75:25) to obtain compound **3** (3.9 mg). Fr 7 (2.1 g) was subsequently chromatographed on a silica gel CC (300 g, 4 × 60 cm) eluted with *n*-hexane–(CH₃)₂CO (65:35) and followed by increasing concentrations of 1-propanol (2%) to give four subfractions (Fr.7.1–Fr.7.4). Fr.7.3 (400 mg) was applied to a

silica gel column (100 g, 2.0 × 80 cm) and eluted with *n*-hexane-CHCl₃-MeOH (47:47:6) to give six subfractions (Fr.7.3.1–Fr.7.3.6). Fr.7.3.6 (40 mg) was separated by preparative reversed-phase HPLC using the mobile phase of MeCN-H₂O (55:45, v/v) to yield compound **2** (1.6 mg).

Compound 1 Yellow gum, $[\alpha]_D^{25} + 17.2$ ($c = 1.0$, CH₃OH); HR-ESIMS $[M + H]^+$ m/z 535.3067 (calcd for C₃₃H₄₃O₆, 535.3054); ¹H and ¹³C NMR data in Table 1.

Compound 2 White powder, $[\alpha]_D^{25} + 30.5$ ($c = 1.0$, CHCl₃); HR-ESIMS $[M + H]^+$ m/z 413.1941 (calcd for C₂₄H₂₉O₆, 413.1959); ¹H and ¹³C NMR data in Table 1.

Compound 3 Colorless oil, $[\alpha]_D^{25} + 9.1$ ($c = 1.0$, CH₃OH); HR-ESIMS $[M + Na]^+$ m/z 293.1366 (calcd for C₁₄H₂₂O₅Na, 293.1365); ¹H and ¹³C NMR data in Table 2.

X-ray crystallographic analysis of 2. C₂₄H₂₈O₆, colorless prism, 0.20 × 0.08 × 0.05 mm, space group P2₁2₁2₁, orthogonal, $a = 6.8847(4)$ Å, $b = 15.1910(16)$ Å, $c = 20.6691(14)$ Å, $V = 2161.7(3)$ Å³, $Z = 4$, $\rho_{\text{calcd}} = 1.267$ g·cm⁻³, $T = 173$ K, Cu radiation ($\lambda = 1.54184$ Å), θ range 3.6°–62.1°, 5988 reflections collected, 3323 independent, $R_{\text{int}} = 0.0708$, 308 parameters, $wR2 = 0.1110$ (all data), $R1 = 0.0512$ [$I > 2\sigma(I)$], absolute structure parameter 0.0(2). The crystal data of compound **2** was placed in the Cambridge Crystallographic Data Centre (CCDC 1992711).

ECD calculations of 1 and 3. Conformational analysis of compounds **1** and **3** was carried out on Macro-Model 9.1 software by applying OPLS-2005 force field in H₂O (Schrödinger LLC) with the Gaussian 09 program package³¹, and ECD curves were obtained using SpecDis version 1.64³².

In vitro antiprotozoal assay. The in vitro inhibitory activities of compounds **1–3** were evaluated against the protozoan parasites *T. b. rhodesiense* (STIB900) trypomastigotes and *P. falciparum* (NF54) LEF stage and cytotoxicity in L6 cells (rat skeletal myoblasts) by adopting the same procedures as the reported previously^{33,34}.

Received: 22 August 2020; Accepted: 7 December 2020

Published online: 14 January 2021

References

1. Tanaka, N. *et al.* Biyouyanagin A, an anti-HIV agent from *Hypericum chinense* L. var. *salicifolium*. *Org. Lett.* **7**, 2997–2999 (2005).
2. Henry, G. E. *et al.* Acylphloroglucinol derivatives from *Hypericum prolificum*. *J. Nat. Prod.* **69**, 1645–1648 (2006).
3. Nürk, N. M. & Blattner, F. R. Cladistic analysis of morphological characters in *Hypericum* (Hypericaceae). *Taxon* **59**, 1495–1507 (2010).
4. Zhang, J.-J. *et al.* Hypercohones D–G, new polycyclic polyprenylated acylphloroglucinol type natural products from *Hypericum cohaerens*. *Nat. Prod. Bioprospect.* **4**, 73–79 (2014).
5. Tanaka, N., Abe, Sh., Hasegawa, K., Shiro, M. & Kobayashi, J. Biyoulactones A–C, new pentacyclic meroterpenoids from *Hypericum chinense*. *Org. Lett.* **13**, 5488–5491 (2011).
6. Fobofou, S. A. T., Franke, K., Porzel, A., Brandt, W. & Wessjohann, L. A. Tricyclicacylphloroglucinols from *Hypericum lanceolatum* regioselective synthesis of selancins A and B. *J. Nat. Prod.* **79**, 743–753 (2016).
7. Cardona, L., Pedro, J. R., Serrano, A., Munoz, M. C. & Solans, X. Spiroterpenoids from *Hypericum reflexum*. *Phytochemistry* **33**, 1185–1187 (1993).
8. Tanaka, N. *et al.* Acylphloroglucinol, biyouyanagiol, biyouyanagin B, and related spiro lactones from *Hypericum chinense*. *J. Nat. Prod.* **72**, 1447–1452 (2009).
9. Zhu, H. *et al.* Hyperascryones A–H, polyprenylated spirocyclic acylphloroglucinol derivatives from *Hypericum ascyron* Linn. *Phytochemistry* **115**, 222–230 (2015).
10. Hu, L. *et al.* (±)-Japonones A and B, two pairs of new enantiomers with anti-KSHV activities from *Hypericum japonicum*. *Sci. Rep.* **6**, 27588 (2016).
11. Schiavone, B. I. *et al.* Biological evaluation of hyperforin and hydrogenated analogue on bacterial growth and biofilm production. *J. Nat. Prod.* **76**, 1819–1823 (2013).
12. Li, D. *et al.* Two new adamantyl-like polyprenylated acylphloroglucinols from *Hypericum attenuatum* choisy. *Tetrahedron Lett.* **56**, 1953–1955 (2015).
13. Tanaka, N. *et al.* Xanthenes from *Hypericum chinense* and their cytotoxicity evaluation. *Phytochemistry* **70**, 1456–1461 (2009).
14. Ghasemi Pirbalouti, A., Jahanbazi, P., Enteshari, S. H., Malekpoor, F. & Hamed, B. Belgrade. *Arch. Biol. Sci.* **62**, 633–642 (2010).
15. Matsuhisa, M. *et al.* Benzoylphloroglucinol derivatives from *Hypericum scabrum*. *J. Nat. Prod.* **65**, 290–294 (2002).
16. Matsuhisa, M. *et al.* Prenylated benzophenones and xanthenes from *Hypericum scabrum*. *J. Nat. Prod.* **65**, 290–294 (2004).
17. Gao, W. *et al.* Polycyclic polyprenylated acylphloroglucinols congeners from *Hypericum scabrum*. *J. Nat. Prod.* **79**, 1538–1547 (2016).
18. Gao, W. *et al.* Polyisoprenylated benzoylphloroglucinol derivatives from *Hypericum scabrum*. *Fitoterapia* **115**, 128–134 (2016).
19. Ciochina, R. & Grossman, R. B. Polycyclic polyprenylated acylphloroglucinols. *Chem. Rev.* **106**, 3963–3986 (2006).
20. Moridi Farimani, M. *et al.* Hydrangenone, a new isoprenoid with an unprecedented skeleton from *Salvia hydrangea*. *Org. Lett.* **14**, 166–169 (2012).
21. Moridi Farimani, M. *et al.* Phytochemical study of *Salvia lerrifoliaroots*: rearranged abietane diterpenoids with antiprotozoal activity. *J. Nat. Prod.* **81**, 1384–1390 (2018).
22. Tabefam, M. *et al.* Antiprotozoal isoprenoids from *Salvia hydrangea*. *J. Nat. Prod.* **81**, 2682–2691 (2018).
23. Tian, W.-J. *et al.* Dioxasampsones A and B, two polycyclic polyprenylated acylphloroglucinols with unusual epoxy-ring-fused skeleton from *Hypericum sampsonii*. *Org. Lett.* **16**, 6346–6349 (2014).
24. Yang, X.-W. *et al.* Polyprenylated acylphloroglucinols congeners possessing diverse structures from *Hypericum henryi*. *J. Nat. Prod.* **78**, 885–895 (2015).
25. Piccinelli, A. L. *et al.* Structural revision of clusianone and 7-epi-clusianone and anti-HIV activity of polyisoprenylated benzophenones. *Tetrahedron* **61**, 8206–8211 (2005).

26. Taylor, W. F. *et al.* 7-epi-Clusianone, a multi-targeting natural product with potential chemotherapeutic, immune-modulating, and anti-angiogenic properties. *Molecules* **24**, 4415 (2019).
27. George, J., Hesse, M. D., Baldwin, J. E. & Adlington, R. M. Biomimetic syntheses of polycyclic polyprenylated acylphloroglucinol natural products isolated from *Hypericum papuanum*. *Org. Lett.* **15**, 3532–3535 (2010).
28. Tseng, Y.-J. *et al.* Lochmolins A-G, new sesquiterpenoids from the soft coral *Simularia lochmodes*. *Mar. Drugs* **10**, 1572–1581 (2012).
29. Huong, N.-T. *et al.* Eudesmane and aromadendrane sesquiterpenoids from the Vietnamese soft coral *Simularia erecta*. *Nat. Prod. Res.* **32**, 1798–1802 (2018).
30. Tabatabaei, S. M. *et al.* Antiprotozoal germacranolide sesquiterpene lactones from *Tanacetum sonbolii*. *Planta Med.* **85**, 424–430 (2019).
31. Frisch, M. J. *et al.* *Gaussian 09, Revision D. 01* (Gaussian, Inc., Wallingford, CT, 2009).
32. Bruhn, T., Schaumlöffel, A., Hemberger, Y. & Bringmann, G. SpecDis: Quantifying the comparison of calculated and experimental electronic circular dichroism spectra. *Chirality* **25**, 243–249 (2013).
33. Orhan, I., Şener, B., Kaiser, M., Brun, R. & Tasdemir, D. Inhibitory activity of marine sponge-derived natural products against parasitic protozoa. *Mar. Drugs* **8**, 47–58 (2010).
34. Zimmermann, S., Kaiser, M., Brun, R., Hamburger, M. & Adams, M. The first plant natural product with *in vivo* activity against *Trypanosoma brucei*. *Planta Med.* **78**, 553–556 (2012).

Acknowledgements

Financial supports by the Golestan and Shahid Beheshti Universities Research Councils are gratefully acknowledged.

Author contributions

M.M.F. designed and coordinated the project. S.S. performed the extraction, isolation and structural identification of the compounds. M.A., M.T. and O.D. helped with the experimental procedures. T.G. conducted the X-ray crystal structure analysis. S.N.E. calculated the ECD data. M.K. carried out the biological assays. M.H. and H.S. provided the instrumental facilities and edited and polished the manuscript. S.S., M.A. and M.M.F. wrote the manuscript. All authors reviewed the manuscript.

Competing interests

The authors declare no competing interests.

Additional information

Supplementary Information The online version contains supplementary material available at <https://doi.org/10.1038/s41598-020-79305-y>.

Correspondence and requests for materials should be addressed to M.M.F.

Reprints and permissions information is available at www.nature.com/reprints.

Publisher's note Springer Nature remains neutral with regard to jurisdictional claims in published maps and institutional affiliations.



Open Access This article is licensed under a Creative Commons Attribution 4.0 International License, which permits use, sharing, adaptation, distribution and reproduction in any medium or format, as long as you give appropriate credit to the original author(s) and the source, provide a link to the Creative Commons licence, and indicate if changes were made. The images or other third party material in this article are included in the article's Creative Commons licence, unless indicated otherwise in a credit line to the material. If material is not included in the article's Creative Commons licence and your intended use is not permitted by statutory regulation or exceeds the permitted use, you will need to obtain permission directly from the copyright holder. To view a copy of this licence, visit <http://creativecommons.org/licenses/by/4.0/>.

© The Author(s) 2021